DOI: 10.13009/EUCASS2019-103

DOI: 103

Diffusion Effects on Catalytic Measurements in Plasma Wind Tunnels

A. Viladegut⋆† *and O. Chazot*⋆
⋆*von Karman Institute for Fluid Dynamics*
72, Chaussée de Waterloo, BE-1640 - Rhode-Saint-Genèse, Belgium
alan.viladegut@vki.ac.be · olivier.chazot@vki.ac.be
†Corresponding author

Abstract

This work provides catalytic recombination coefficients (γ) on water-cooled copper calorimeters at 350 K. Measurements are obtained on probes of different sizes, tested in a plasma wind tunnel at stagnation point configuration. Despite pressure and surface temperature are the same among the probes, different catalytic activities are observed. This fact is not consistent with γ-models implemented in CFD solvers, which assume catalytic recombination of first order. A dimensional analysis shows that data is consistent with theoretical work of Rosner, and that different levels of gaseous recombination can influence the empirical determination of γ.

1. Introduction

The recovery of a payload orbiting a planet requires a space vehicle ready to withstand the harsh thermal and chemical environments encountered during re-entry. For such purpose, the carrier vehicle must be equipped with a Thermal Protection System (TPS) that not only insulates the payload from the hot plasma surrounding the vehicle, but also provides the structural integrity for a safe and optimized landing.

Different strategies can be followed during the development of a TPS, depending on the mission profile. For instance, using a material that ablates under hot and dissociated gases can be very efficient for fast re-entries. This is the case of most ballistic entries, in which TPS materials react with the gas species and they are depleted during the flight, leading to wall recession on the vehicle's surface. Under other circumstances, however, the goal is the re-usability of the carrier vehicle. This is typical of lifting body entries, whose flight duration is longer and heating conditions are not as severe as in ballistic entries. In this case, TPS materials are inert to the gas. However, despite the fact that re-usable TPS material surfaces remain unchanged during the re-entry process, it does not imply that they do not interact chemically with the gas. In fact, these materials can catalyze atomic recombination from gaseous species and release energy close to the vehicle's surface, increasing significantly the heating of the vehicle. Therefore, for re-usable TPS design, low catalytic materials are of most interest for safe and efficient missions.

The accurate characterization of catalytic phenomena on material surfaces is critical for the design of re-usable TPS. The recombination coefficient γ is the reference parameter to quantify the catalytic activity on surfaces. Goulard[9] introduced γ in aerospace activities as the ratio between the flux of atomic species i recombining ($N_{i,r}$) and the total atomic flux of atoms impinging on a catalytic surface (N_i), and defined the coefficient as:

$$\gamma_i = \frac{N_{i,r}}{N_i} = k_{w,i}\sqrt{\frac{2\pi m_i}{k_B T_w}} \tag{1}$$

where $k_{w,i}$ is the reaction rate constant, k_B is Boltmann's constant, m_i is the particle mass of species i, and T_w is the temperature at the surface. Note that, if the catalytic reaction is assumed of first order, the reaction rate constant can be modelled as an Arrhenius function and γ becomes a parameter that depends only on T_w. This is a relevant fact to keep in mind for the discussion below.

The empirical determination of the recombination coefficient is of paramount importance to define proper boundary conditions for the species equations in non-equilibrium Computational Fluid Dynamic (CFD) simulations, and to con-

DOI: 10.13009/EUCASS2019-103

tribute on the prediction of heating during the TPS design. Plasma wind tunnels are conceived to reproduce the thermal and chemical conditions that take place behind the shock wave appearing in hypersonic flights, and for that, they are well positioned to test TPS material candidates under conditions that are close to re-entry flight. The Plasmatron facility at the von Karman Institute (VKI) is an Inductively Couple Plasma (ICP) facility that has been extensively used to characterize the catalytic activity on both metallic and ceramic TPS materials.[14] Data of recombination coefficients measured in other facilities is also available in literature.[1–3,6]

Despite a broad range of data for catalytic recombination coefficients exists, recent experiments in the VKI-Plasmatron suggest that the catalytic phenomena can not be fully described by Eq. 1. In those experiments, the recombination coefficients on copper caloremeters at 350 K were determined at both stagnation and off-stagnation point configurations. In the two situations, lower values of γ were observed at higher static pressure settings of the Plasmatron chamber.[17] Moreover, tests showed that γ transitions from high-catalytic to low-catalytic as particles flow downstream of a linear calorimeter inserted in a flat plate model.[18] Data from those experiments are provided in Fig. 1 and Fig. 2, respectively. Results suggest that the empirical determination of γ in plasma wind tunnels is affected by other flow properties different than T_w, and such conclusion is not aligned with the first order reaction hypothesis introduced by Goulard in Eq. 1. Therefore, an inconsistency exists between what is measured in plasma wind tunnels, and what is actually implemented in CFD tools.

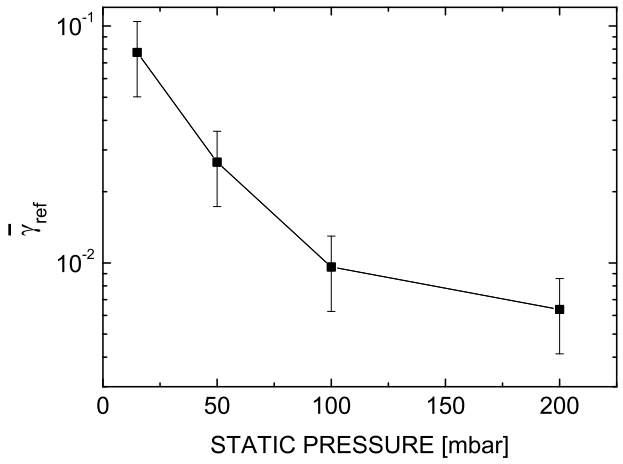

Figure 1: Recombination coefficients on copper calorimeter determined at different pressures in Plasmatron chamber.[17]

The present work extends the investigation further through new experiments in Plasmatron. They are focused on the determination of γ around three different probes holding a copper calorimeter. Calorimeters are tested under the same plasma free-stream conditions and equal T_w (350 K), but under different conditions of chemical non-equilibrium for the boundary layer. Interestingly, although new data remains incompatible with the first order reaction hypothesis, results are consistent with previous theoretical formulations of boundary layer equations that considered species diffusion due to gaseous reactions. As consequence, measurements provided here, allow building a strategy to relate experimental data to values used in CFD. The work concludes that measurements of γ in plasma wind tunnels only apply to specific flight situations through an extrapolation technique capable of matching the two environments.

2. On the catalysis determination in non-equilibrium flows

To illustrate the problem regarding catalytic measurements under non-equilibrium boundary layers, it is worth considering the work of Rosner,[15] in which Broadwell's conductivity cell model[7] is generalized to include first order atom recombination at a cold surface of arbitrary catalytic activity. The flow within two parallel plates separated by a distance δ and enclosing a partially dissociated gas is analyzed. One of the plates is hot and under Local Thermodynamic Equilibrium (LTE) conditions, whereas the other one is cold and with finite catalytic properties.

DOI: 10.13009/EUCASS2019-103

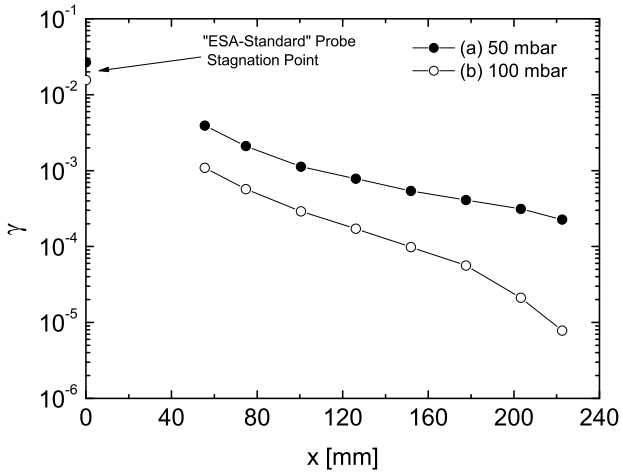

Figure 2: Recombination coefficients on copper determined along a linear calorimeter inserted in a flat plate model.[18]

Three non-dimensional parameters appear in the problem:

- Damköhler in the gas (Da_g): it is defined here as the ratio between the characteristic diffusion time δ^2/D_{12} and the characteristic chemical relaxation time τ_{chem}. It defines the level of non-equilibrium for the gaseous reactions. The lower limit is set by $Da_g \rightarrow 0$, meaning that chemistry is “slow" and the flow remains chemically frozen; whereas the upper limit is defined by $Da_g \rightarrow \infty$, where the composition of the gas relaxes “instantly" to the temperature and pressure conditions of the gas and the flow is in chemical equilibrium. Finite values of Da_g means that the flow is in chemical non-equilibrium.

- Damköhler at the wall (Da_w): it is the ratio between the characteristic diffusion time δ/D_{12} and the characteristic chemical relaxation time for the catalytic reaction, which, in turn, is inversely proportional to k_w. The lower limit is set by $Da_w \rightarrow 0$, meaning that catalytic reactions are not relevant to the flow, and the problem remains reaction-limited. The upper limit is defined by $Da_w \rightarrow \infty$, meaning that particles do not diffuse at enough speed in order to feed the catalytic reaction at the surface, leading to a boundary layer that is diffusion-limited.

- Enthalpy parameter (H): is a measure of the maximum possible enthalpy change $\Delta h_{chem,eq}$ across the cell as compared to the enthalpy change under frozen conditions Δh_{fr} for the given temperature difference $T_{hot} - T_{cold}$ imposed by the two plates. H includes as multiplier a recovery factor r_D for chemical energy, which is function of the Lewis number for stagnant flows.

  The Nusselt number (Nu) based on the temperature change between the plates across the film thickness δ is:

$$Nu = 1 + \phi H \tag{2}$$

where ϕ is defined as:

$$\phi = 1 - \left\{ 1 + Da_w - \frac{1 - \xi coth\xi}{1 + H} \right\}^{-1} \tag{3}$$

and $\xi = \sqrt{Da_g(1+H)}$. The surface $Nu = f(Da_g, Da_w)$ provided by Rosner is shown in Fig. 3 for $H = 9$. As expected, the heat flux transferred to the cold wall increases with both Damköhler numbers. However, one may realize that for large Da_g, there are less atoms available close to the surface due to the presence of gaseous recombination, leading to a heat flux that is less sensitive to the wall catalytic reactions. This fact could have an important consequence when determining a catalytic recombination coefficient based on calorimetric measurements in plasma wind tunnels because uncertainties associated with measuring instruments, data processing and chemical models may lead to an experimentally determined catalytic activity that falsely appears influenced by many flow parameters instead of only the surface temperature. This is the reason why the preferred conditions for catalysis determination are under very low pressure environments, where collisions between atoms is unlikely to occur and the frozen flow conditions are achieved.

DOI: 10.13009/EUCASS2019-103

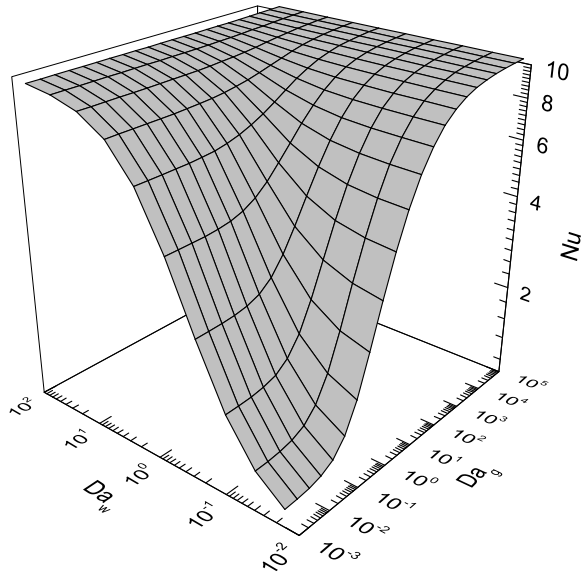

Figure 3: Nu number as a function of Da_g and Da_w for $H = 9$, as proposed by Rosner.[15]

The peak heating conditions of a space vehicle re-entering the atmosphere normally occurs at intermediate altitudes, where pressure conditions are excessively high to provide a chemically frozen flow. Plasma wind tunnels are designed to operate at such pressure levels, and for that, frozen environments are only attained in the test chamber for a small area of their test envelope.

Therefore, the experimentally determined recombination coefficient in a plasma wind tunnel should be regarded as a function of the particular combination of Da_g, Da_w, Nu and H, which corresponds to only one specific test condition in a plasma wind tunnel. This means that there is a role of the species diffusion inside the boundary layer, ruled by the relative relevance of both gaseous and heterogeneous reactions with respect to the flow velocity, that can affect the chemical contribution to the heat flux. As consequence, any recombination coefficient determined through a heat flux measurement could appear influenced by different boundary layer diffusion properties, falsifying the values that should be actually considered in CFD.

3. The VKI-Plasmatron facility

The VKI-Plasmatron is a 1.2 MW ICP facility that uses 2 kV at 400 kHZ to create and expand the plasma into a 2.5 m long and 1.4 m diameter test chamber through a 160 mm diameter torch. A scheme of the facility is provided in Fig. 4. It can operate with different gases at both subsonic and supersonic regimes, with air, N_2 and CO_2 being the most commonly used. Test samples are normally located 445 mm from the torch exit. This is a standard configuration for most of the subsonic tests, adopted also in the present work. A heat exchanger is placed behind the chamber and is connected to a cooling system to ensure the appropriate gas temperature reduction before particles reach the vacuum pumps. Remark also that all metallic surfaces exposed to plasma are cooled down with water to prevent them from melting.

Pressure ports allow different pressure measurements. Static pressure P_s is measured at the top of the chamber with an absolute pressure transducer (Membranovac DM 12, Leybold Vacuum, OC Oerlikon Corporation AG, Switzerland) with ±0.7 hPa accuracy. Dynamic pressure P_{dyn} is taken with a variable reluctance pressure transducer (DP-15, Valydine Engineering Corp, Northridge, CA USA) of ±0.2% uncertainty. One of its ports is connected to the stagnant flow through a pitot probe, while the other has access to the static pressure line. It is assumed that uncertainties increase to ±10% for P_s due to the stability of the pumps regulating the vacuum conditions and to ±20% for P_{dyn} due to plasma jet fluctuations.[14] The gas mass flow rate is normally set at 16 g/s and controlled with a rotameter.

DOI: 10.13009/EUCASS2019-103

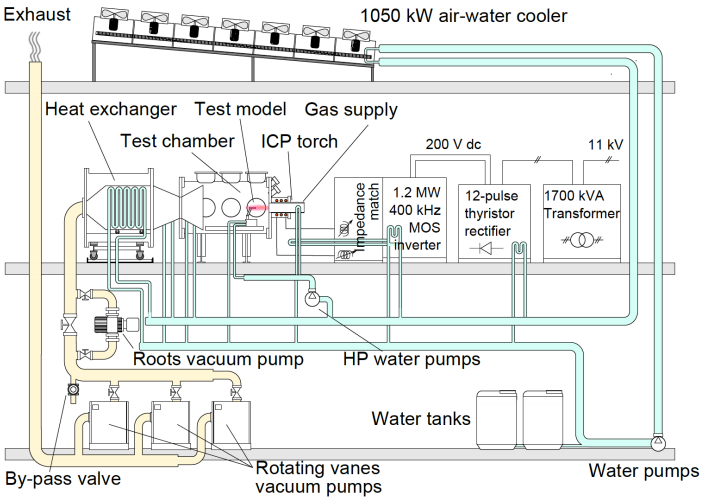

Figure 4: The VKI-Plasmatron facility.

3.1 The Damköhler probes

The three Damköhler probes shown in Fig. 5 are available in the VKI to take stagnation point measurements under different chemical regimes. The design of these probes was presented by Herpin[11] when studying the scaling of chemistry in non-equilibrium flows. Dimensions of each probe are specified in Table 1, with R_b being the probe main radius and R_c the radius of the edge. The three probes are water-cooled and made of copper. They feature a central bore to house the calorimeter shown in Fig. 6. This calorimeter is water-cooled and temperatures at the inlet and outlet are measured by thermocouples to compute the heat flux transferred from the plasma. The cooling system of both the holder and the calorimeter are insulated from each other with the Teflon ring, also shown in Fig. 6.

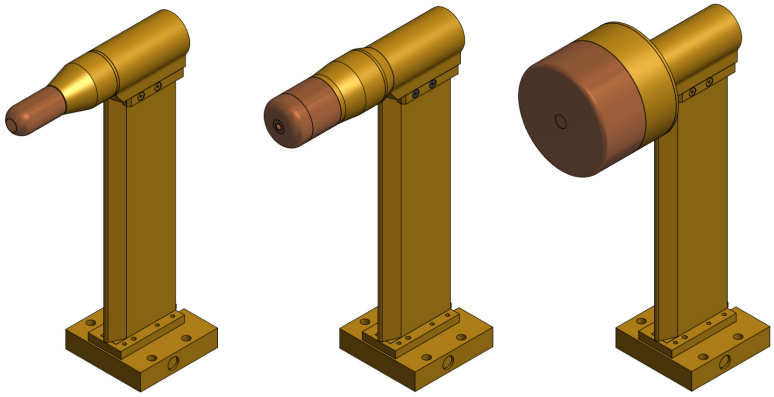

(a) Frozen (FR) (b) Standard (ST) (c) Equilibrium (EQ)

Figure 5: The VKI Damköhler probes.

Table 1: Dimensions of the Damköhler probes

Probe	**Symbol**	R_b, **mm**	R_c, **mm**
Standard	ST	25	11.75
Equilibrium	EQ	57.5	5
Frozen	FR	15	15

DOI: 10.13009/EUCASS2019-103

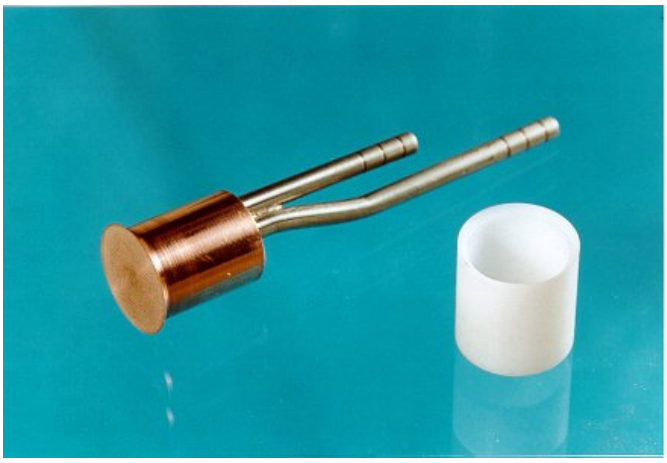

Figure 6: Copper calorimeter inserted in Damköhler probes.

The ESA-Standard probe, identified as ST in Fig. 5, is used as reference to determine the free-stream enthalpy conditions of Plasmatron through a non-equilibrium boundary layer solver (CERBOULA) developed by Barbante.[4] The reference catalytic model used for enthalpy rebuilding was developed by the authors[17] and it is provided in Fig. 1. The other two probes either promote or hamper the gaseous recombination when compared to the reference configuration. The concept behind the design of these three probes consists on changing Da_g between them, while keeping the same plasma free-stream conditions. The fact is, increasing the size of the probe leads to a thicker boundary layer, making the diffusion zone larger and providing the gas more time to recombine. Thus, the larger holder is known as the Equilibrium probe because it increases Da_g when compared to the Standard probe. Conversely, the smaller probe is named Frozen probe because it tends to decrease the Da_g.

The Damköhler probes were already used by Krassilchikoff[13] in the so-called "Equilibrium flow extrapolation". Unfortunately, that test campaign was not fully successful. Then, de Crombrugghe[8] measured catalysis on both the Frozen and the Equilibrium probes to investigate qualitatively the behavior of gas-surface interaction phenomena under different Da_g regimes in the context of the Local Heat Transfer Simulation (LHTS) methodology. Additional tests were carried out by Panerai[14] on C/SiC samples using both the Standard and the Equilibrium probes. He showed how different probe geometries led to different values of γ on the same material. However, since the surface temperature on C/SiC was not the same among different probes, the non-equilibrium effect on the determination of γ could not be properly assessed. Actually, the main difference with the campaign presented below is the control of T_w on the calorimeters. The fact is, surface temperatures on TPS materials can differ by several hundreds of degrees from one probe to another, whereas it is reasonable to assume that the surface of a water-cooled calorimeter remains at 350 K for any probe configuration.

In order to illustrate the influence of the probe design on the boundary layer chemical non-equilibrium properties, examples of both atomic oxygen and nitrogen mass fractions profiles computed with CERBOULA for the three Damköhler probes are shown in Fig. 7. They are obtained under the same plasma conditions of temperature and pressure, and the non-catalytic assumption is prescribed so that species profiles are consequence of gaseous recombination only. As expected, the Frozen probe leads to a thinner chemical boundary layer when compared to both the Standard and the Equilibrium probes. The effect of the probe geometry on the amount of recombination is clear if one observes the N profiles among the three probes. It is observed that the mass fraction at the wall of the Equilibrium probe is significantly lower than the value computed for the Frozen probe, with the mass fraction at the wall of the Standard probe falling in between. The O-atom profile, on the other hand, remains almost frozen and fully dissociated for the three probes. Figure 7 also demonstrates that non-equilibrium boundary layers are present with any probe configuration, meaning that the size of the probe favors either frozen or equilibrium regimes, but it cannot enforce the development of purely frozen ($Da_g \to 0$) or purely equilibrium ($Da_g \to \infty$) boundary layers.

DOI: 10.13009/EUCASS2019-103

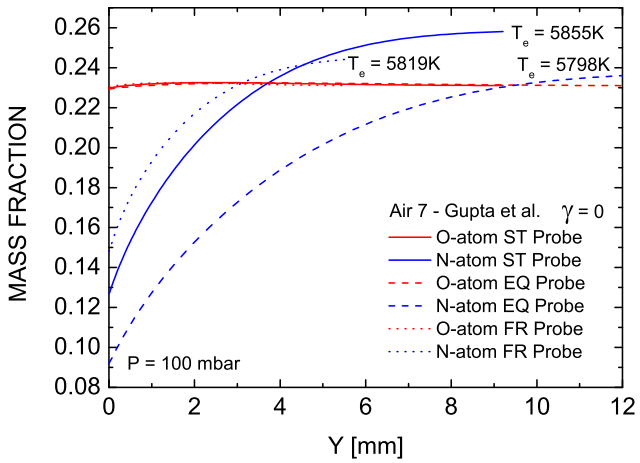

Figure 7: Example of the O and N profiles among the Damköhler probes for the same testing conditions of temperature and pressure and a non-catalytic wall.

4. Catalysis determination at stagnation point

A test campaign is carried out in the Plasmatron to address the possible relation between the chemical non-equilibrium characteristics of the boundary layer and the wall catalysis determined in a plasma wind tunnel. To this end, the three Damköhler probes are exposed to the same plasma conditions of enthalpy H_e, mass flow of air $\dot{m}$ and static pressure P_s, as illustrated by the sketch of Fig. 8. The probes are installed at 445 mm downstream from the torch exit, and they are aligned with the core of the jet. The Standard and the Equilibrium holders are installed on the lower injection system, whereas the Frozen holder is installed on the upper one, at the top of the chamber.

A copper calorimeter is inserted at the center of each probe. The mass flow of water that is circulating inside each calorimeter is kept constant using rotameters once they are exposed to plasma, and its temperature difference between the inlet and the outlet is measured with pairs of E-thermocouples. The computation of the heat flux is carried out in real time by the data acquisition system and recorded at 1 Hz.

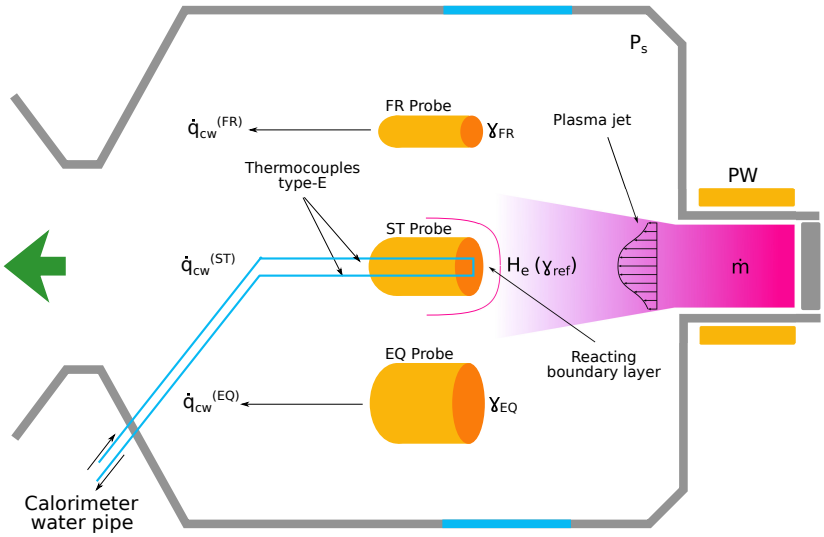

Figure 8: Plasmatron test configuration for catalysis determination on the Damköhler probes.

A test matrix with 9 power levels and 2 chamber pressure conditions (50 and 100 mbar) is considered. The mass flow

DOI: 10.13009/EUCASS2019-103

rate of air entering the Plasmatron chamber is set constant at 16 g/s, and the power applied to the coil PW is varied according to the target heat flux conditions on the Standard probe, which is used as reference to define H_e during the post processing with CERBOULA. Time-averaged heat flux measurements on the three probes are listed in Table 2, together with the target condition $\dot{q}_{cw}^{(ref)}$ and PW.

Table 2: Heat flux measurements during the Damköhler probes test campaign: b)50 mbar; c)100 mbar

Test	$\dot{q}_{cw}^{(ref)}$ **kW m^{-2}**	PW **kW**	$\dot{q}_{cw}^{(ST)}$ **kW m^{-2}**	$\dot{q}_{cw}^{(FR)}$ **kW m^{-2}**	$\dot{q}_{cw}^{(EQ)}$ **kW m^{-2}**
1b	300	125	297.10	401.79	74.84
2b	500	148	464.09	541.82	107.97
3b	700	168	666.64	789.66	231.35
4b	900	187	862.94	1047.18	380.45
5b	1100	244	1070.71	1306.58	459.41
6b	1300	252	1327.23	1492.22	665.90
7b	1500	278	1496.27	1750.11	841.29
8b	1700	297	1708.32	2083.47	1048.70
9b	2000	323	2018.90	2315.14	1214.37
1c	300	136	276.64	344.27	104.35
2c	500	145	524.24	629.82	254.24
3c	700	187	673.32	1059.45	419.42
4c	900	192	926.48	1100.61	565.62
5c	1100	225	1099.08	1360.03	594.82
6c	1300	266	1286.49	1773.63	807.58
7c	1500	276	1490.70	1826.35	886.47
8c	1700	300	1678.81	2059.42	1050.43
9c	2000	330	1967.04	2377.24	1279.21

Due to the fact that only three probes can be installed in the Plasmatron chamber at the same time, the dynamic pressure measurements could not be taken during the same Plasmatron run. Instead, they are measured in a separate test campaign that targets the same testing conditions as those used for the Damköhler probes. With the purpose of matching consistently the heat flux measurements and the dynamic pressure data with the same target condition, a linear regression of the form $\dot{q}_{cw}^{(i)} = y_0 + m\dot{q}_{cw}^{(ref)}$ is carried out on all the measured quantities using the heat flux on the Standard probe as reference. The resulting coefficients of such approximation are provided in Table 3, together with the coefficient of determination R^2 of the fit.

Table 3: Linear interpolation coefficients for the heat fluxes measured on the Damköhler probes ($\dot{q}_{cw}^{(i)} = y_0 + m\dot{q}_{cw}^{(ref)}$)

P_s	**Probe (i)**	y_0	m	$\mathbf{R^2}$
50 mbar	FR	40.1462	1.1467	0.9953
50 mbar	EQ	-211.53	0.6990	0.9851
50 mbar	Pitot	-10.389	0.0810	0.9339
100 mbar	FR	77.888	1.1922	0.9784
100 mbar	EQ	-83.697	0.6768	0.9911
100 mbar	Pitot	-7.320	0.0340	0.9672

Then, the reference heat flux measurement, combined with γ_{ref} of Fig. 1, provides the outer edge enthalpy for the 18 testing conditions using CERBOULA. Once the free-stream conditions are defined, the same code can be used around the Frozen and the Equilibrium probes to determine γ_{FR} and γ_{EQ}, respectively. Note that the chemical model proposed by Gupta et al.[10] is used for post-processing. Results are shown and discussed in the section below for each pressure condition.

DOI: 10.13009/EUCASS2019-103

5. Catalysis determination and dimensional analysis

5.1 Analysis of the Damköhler probes at 50 mbar

Results for H_e, γ and δ at 50 mbar are listed in Table 4 for the three probes. Note that, although the recombination coefficients on the Equilibrium probe could be determined in most of the situations, CERBOULA did not converge at both the lowest and the highest powers of the campaign. The behavior of boundary layer thicknesses is consistent for the three probes. That is $\delta_{FR} < \delta_{ST} < \delta_{EQ}$. Remark that values of δ are rather independent with respect to power for the Standard and the Frozen probes, whereas a maximum difference of 11.31 mm is observed between case 4b and 7b for the Equilibrium probe.

Table 4: H_e, γ and δ at 50 mbar on the Damköhler probes

Test	H_e **MJ kg^{-1}**	γ_{ref}	δ_{ST} **mm**	γ_{FR}	δ_{FR} **mm**	γ_{EQ}	δ_{EQ} **mm**
1b	9.88	0.02661	11.09	0.00948	4.27	-	27.39
2b	13.41	0.02661	10.92	0.00885	4.11	-	23.88
3b	16.88	0.02661	10.64	0.01039	4.04	0.00212	20.94
4b	20.31	0.02661	10.41	0.01165	3.98	0.00490	19.63
5b	23.78	0.02661	10.29	0.01599	3.96	0.00818	20.28
6b	27.48	0.02661	10.32	0.01833	3.94	0.00919	26.18
7b	32.03	0.02661	10.67	0.01834	3.87	0.00874	30.94
8b	36.49	0.02661	11.17	0.01801	3.92	0.01024	29.27
9b	41.36	0.02661	10.79	0.01739	4.55	-	20.80

The recombination coefficients on the Damköhler probes at 50 mbar are shown in Fig. 9 together with γ_{ref}. Error bars around γ_{FR} and γ_{EQ} are computed assuming ±13% uncertainty around H_e, as proposed by Sanson et al.[16] It is observed that both γ_{EQ} and γ_{FR} are lower than γ_{ref}, with γ_{EQ} being the smallest. The recombination coefficient for the Equilibrium probe shows a marked growth for increasing values of H_e. Note that none of the γ_{EQ} error bars cross their γ_{ref} counterparts. Regarding γ_{FR}, it seems that the Frozen and the Standard probes have similar catalytic activities. This influence of H_e on γ was not expected, and it could be caused by the lower dissociation level of nitrogen at low powers.

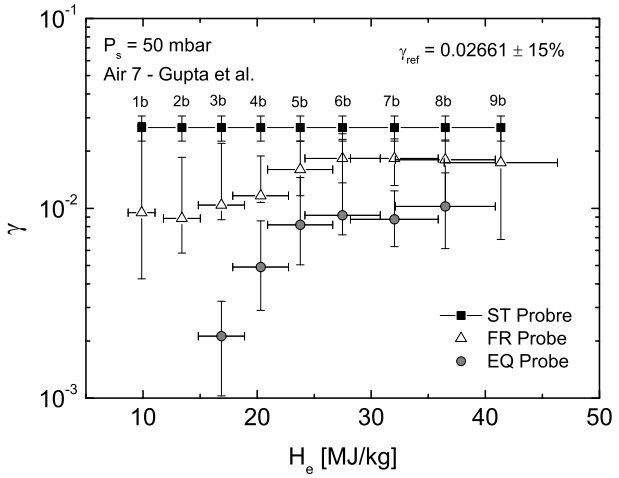

Figure 9: Recombination coefficients on the Damköhler probes at 50 mbar.

In addition, and given the size of each probe, one could have anticipated that values of γ_{ref} would be in between γ_{EQ} and γ_{FR}. However, Fig. 9 shows that this is not the case. The computation of the non-dimensional numbers that

DOI: 10.13009/EUCASS2019-103

intervene in the non-equilibrium characterization of the boundary layer Da_g, Da_w, Nu and H, as explained in Sec. 2, can help understanding such unexpected results. The definition of H for a boundary layer developed in a stagnant flow is:

$$H = Le^{-0.6} \frac{\Delta h_{chem,eq}}{\Delta h_{fr}} \tag{4}$$

where Le is the Lewis number ($Le = \lambda/\rho D c_p$) and it plays the role of a recovery factor for the chemical energy exchange.[15] From Eq. 4, one can conclude that H changes with power, but not among the probes under the same test condition. Therefore, for each Plasmatron test condition (from 1b to 9c), one could draw a different surface $Nu = f(Da_g, Da_w)$, as that shown in Fig. 3, and extract the Nu map plotted in Fig. 10, which is shared between the three probes.

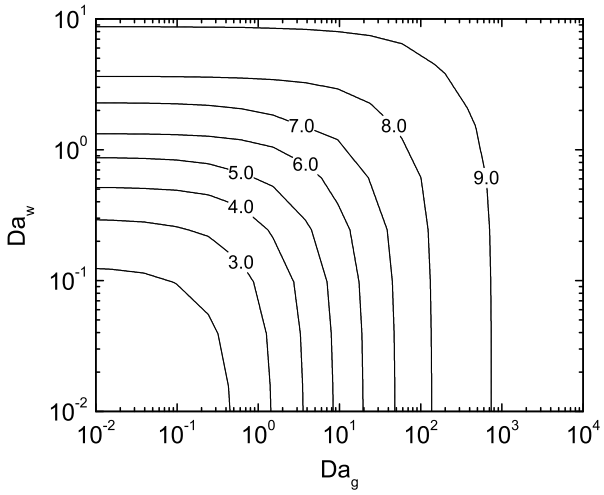

Figure 10: Two-dimensional map of the Nu number as a function of Da_g and Da_w for $H = 9$, as proposed by Rosner.[15]

To proceed with the dimensional analysis, the values of Da_g obtained at 50 mbar are shown in Fig. 11. They are computed as:

$$Da_g = \frac{[\mathrm{N}]\delta^2}{D}\left(4k_f[\mathrm{N}]_{Eq} - k_b\right) \tag{5}$$

considering nitrogen recombination $2\,\mathrm{N} + \mathrm{M} \longrightarrow \mathrm{N_2} + \mathrm{M}$ as reference reaction to estimate the characteristic time of the chemistry, with atomic nitrogen acting as collision partner M. Here, $[N]$ and $[N]_{Eq}$ are the molar fractions of nitrogen in chemical non-equilibrium and in chemical equilibrium, respectively, which are evaluated at half the thickness of the boundary layer together with the diffusion coefficient D. The paremeters k_f and k_b are the forward and backward reaction rate constants that are provided by Gupta et al.[10] chemical model. As expected, Da_g on the Standard probe falls between the values determined for the other two probes, and they all increase with power (or equivalently, the amount of atomic species at the outer edge).

Values of Da_w and Nu at 50 mbar are shown in Fig. 12-Left and Fig. 12-Right, respectively. It is observed that $Da_w^{(FR)} < Da_w^{(ST)}$ and $Nu^{(FR)} < Nu^{(ST)}$, which is consistent with the fact that $Da_g^{(FR)} < Da_g^{(ST)}$, following the map of Fig. 10. As consequence $\gamma_{FR} < \gamma_{ST}$ is obtained.

Considering the Equilibrium probe, however, it is observed that $Da_w^{(EQ)} < Da_w^{(ST)}$ from tests 3b to 5b while $Nu^{(EQ)} \approx Nu^{(ST)}$. The relevance of this result lies on the fact that it follows the logic of Fig. 10 and validates the work of Rosner (see Sec. 2). Indeed, increasing Da_g when switching from the Standard to the Equilibrium probe while keeping the same Nu, reduces Da_w and, eventually, leads to a recombination coefficient reduction. Then, it would seem that an increase of gas recombination induced by the Equilibrium probe can be compensated by a reduction of heterogeneous reactions, in order to keep Nusselt number constant.

DOI: 10.13009/EUCASS2019-103

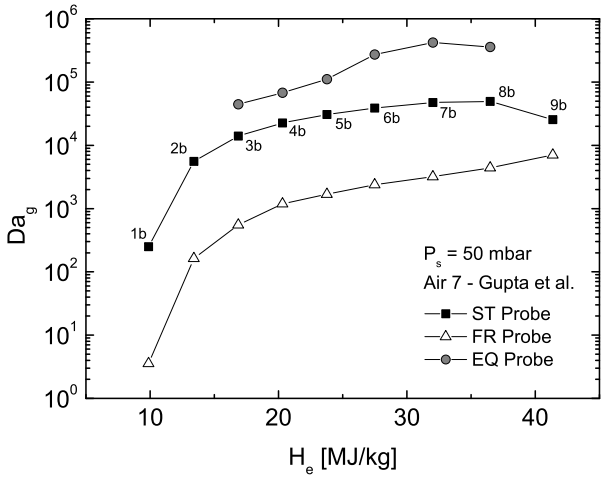

Figure 11: Da_g on the Damköhler probes at 50 mbar.

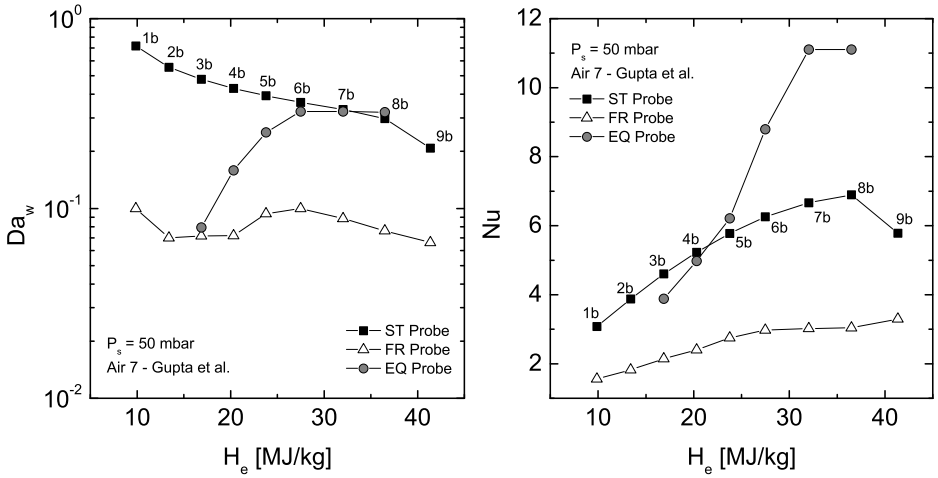

Figure 12: Non-dimensional numbers obtained at 50 mbar: Left - Da_W, Right - Nu

It is also observed that $Da_w^{(EQ)} = Da_w^{(ST)}$ from conditions 6b to 8b and $Nu^{(EQ)} > Nu^{(ST)}$. This is also consistent with Fig. 10 because an increase in Da_g leads to an increase of Nu if Da_w is kept the same, which leads to similar recombination coefficients for the Equilibrium and Standard probes.

From these results, one could conclude that the reduction of the recombination coefficient on both Frozen and Equilibrium probes is consequence of the coupling between Nu, Da_g and Da_w for constant H. This demonstrates the influence of the non-equilibrium environment when experimentally determining the catalytic properties of surfaces.

5.2 Analysis of the Damköhler probes at 100 mbar

The results at 100 mbar are similar to those at 50 mbar and they are provided in Table 5. In this case, CERBOULA did not converge for tests 1c and 9c on the Equilibrium probe. The boundary layer thickness for the Standard and the Frozen probes are similar to those obtained at 50 mbar, whereas they are significantly reduced for the Equilibrium probe. The recombination coefficients are shown in Fig. 13 assuming ±13% uncertainty for H_e and, again, the values on both the Frozen and the Equilibrium probes are lower than γ_{ref}.

DOI: 10.13009/EUCASS2019-103

Table 5: H_e, γ and δ at 100 mbar on the Damköhler probes

Test	H_e **MJ kg^{-1}**	γ_{ref}	δ_{ST} **mm**	γ_{FR}	δ_{FR} **mm**	γ_{EQ}	δ_{EQ} **mm**
1c	11.93	0.00960	10.86	0.00403	4.20	-	24.13
2c	15.10	0.00960	10.60	0.00519	4.01	0.00121	18.92
3c	18.54	0.00960	10.22	0.00628	3.84	0.00243	16.91
4c	22.25	0.00960	9.99	0.00636	3.78	0.00396	15.84
5c	26.02	0.00960	9.83	0.00603	3.74	0.00482	15.09
6c	29.97	0.00960	9.79	0.00651	3.70	0.00480	15.55
7c	34.09	0.00960	9.88	0.00625	3.68	0.00546	17.96
8c	38.07	0.00960	10.22	0.00706	3.60	0.00527	20.57
9c	42.91	0.00960	10.27	0.00479	3.82	-	17.82

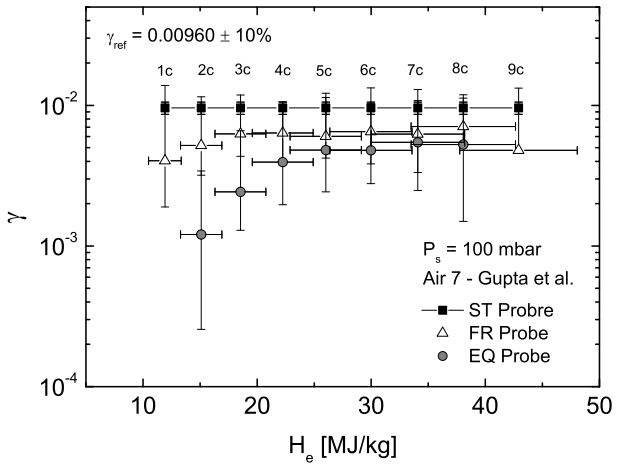

Figure 13: Recombination coefficients on the Damköhler probes at 100 mbar.

Following the same analysis as before, the reduction of the recombination coefficient can be explained with the non-dimensional analysis of different non-equilibrium boundary layers. Again, reducing the size of the probe reduces the computed Da_g and, conversely, a larger probe leads to a higher Da_g, as seen in Fig. 14. In addition, comparing with the results obtained at 50 mbar, rising pressure also increases Da_g due to the higher collision rate between particles.

Both Da_w and Nu at 100 mbar are shown in Fig. 15-Left and Fig. 15-Right. The same conclusions reached at 50 mbar also apply at 100 mbar. For the Frozen probe, a reduction of both Da_g and Nu with respect to the Standard leads to a reduction on Da_w and, consequently, to a lower γ.

For the Equilibrium probe, an increase of Da_g while keeping the same Nu as in the Standard probe, requires $Da_w^{EQ} < Da_w^{ST}$ in order to be consistent with Fig. 10, which results into $\gamma_{EQ} < \gamma_{ref}$ for conditions ranging from 2c to 6c. Therefore, the non-equilibrium influence on the experimentally determined recombination coefficient is also present at 100 mbar.

6. Conclusions

This work provides new recombination coefficient measurements on copper calorimeters at 350 K. They have been tested in Plasmatron faciltiy under different chemical regimes, characterized by finite Damköhler numbers Da. The logic of the experiment is based on the fact that the chemical regime around a sample can be changed through the size of the probe, which imposes certain thickness of the boundary layer. The Frozen and the Equilibrium probes have been designed to either reduce or increase the Da number with respect the Standard probe, which is taken as reference

DOI: 10.13009/EUCASS2019-103

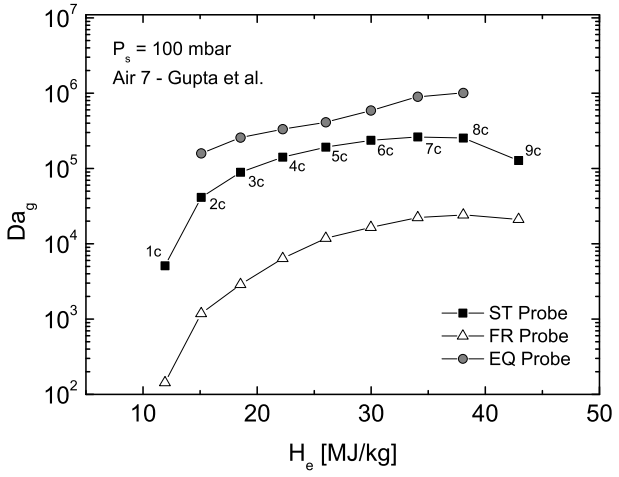

Figure 14: Da_g on the Damköhler probes at 100 mbar.

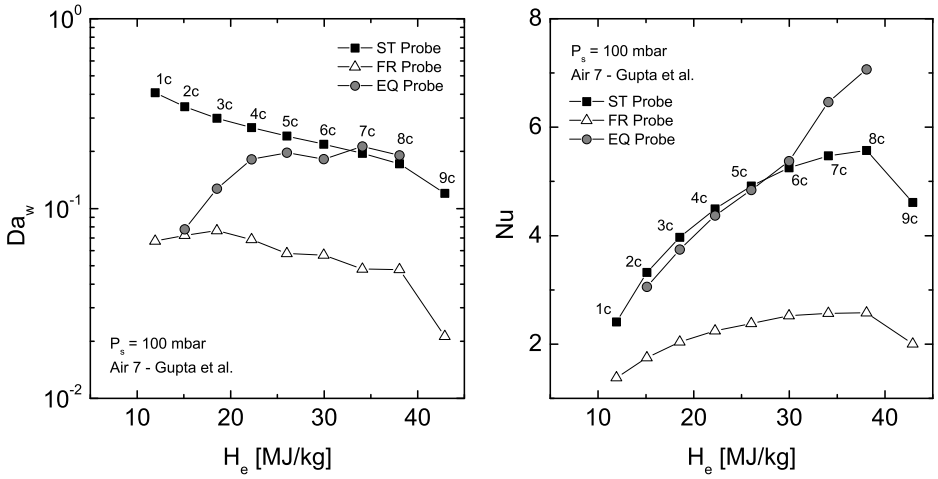

Figure 15: Non-dimensional numbers obtained at 100 mbar: Left - Da_W, Right - Nu

configuration.

However, having a boundary layer in chemical non-equilibrium around a catalytic sample implies that two Da numbers should be considered: one for gaseous reactions (Da_g), and another for catalytic reactions at the surface (Da_w). Differences in γ reported here suggest that a coupling exists between gaseous and heterogeneous reactions. Also, they demonstrate the existence of inconsistencies between catalytic models used in CFD, which assume that catalytic reactions to be of first order, thus implying that γ is only function of T_w.

It is observed that values of γ on both the Frozen (small) and the Equilibrium (large) probes are reduced with respect to a Standard (medium) probe. The dimensional analysis proposed by Rosner has been applied to the experimental data and results are consistent with the theoretical work. Particularly for the Equilibrium probe, it is shown that Da_w is reduced with respect to the Standard probe for the same test condition. This happens at constant Nusselt number and higher Da_g, and such behavior can be explained only by the non-equilibrium boundary layer theory. Therefore, the reduction of γ with respect to the Standard probe can be explained only when the coupling between gaseous and heterogeneous reactions is considered.

This fact implies that, in order to relate experimental data to re-entry vehicle conditions, the same flow topology must

DOI: 10.13009/EUCASS2019-103

be attained in the two situations. As consequence, a flight extrapolation technique shall be applied when using data from plasma wind tunnels to design re-usable TPS and to predict aerodynamic heating around re-entry vehicles.

The Local Heat Transfer Simulation (LHTS) methodology proposed by Kolesnikov[12] allows the stagnation point boundary layer duplication between flight and ground. The methodology states that, the same boundary layer can be obtained in two different configurations, if total pressure, total enthalpy and velocity gradient β at the boundary layer edge in LTE, together with surface temperature and catalycity, are respected between configurations. A CFD analysis provided by Barbante and Chazot[5] shows that the full flow topology is duplicated through LHTS.
Interestingly, the same set of parameters proposed by LHTS can be derived from Da_g, Da_w, Nu and H to define a boundary layer in chemical non-equilibrium. That is, $\delta \propto \beta^{-1}$, $\lambda, D = f(T, P)$ and $k_w \propto \gamma$. Therefore, the works of both Kolesnikov and Rosner actually consider the same independent parameters in the analysis of non-equilibrium boundary layers.

References

[1] M. Balat-Pichelin, J. M. Badie, R. Berjoan, and P. Boubert. Recombination coefficient of atomic oxygen on ceramic materials under earth re-entry conditions by optical emission spectroscopy. *Chemical Physics*, 291:181–194, June 2003.

[2] M. Balat-Pichelin, L. Bedra, O. Gerasimova, and P. Boubert. Recombination of atomic oxygen on α-Al_2O_3 at high temperature under air microwave-induced plasma. *Chemical Physics*, 340:217–226, November 2007.

[3] M. Balat-Pichelin, M. Czerniak, and J.M. Badie. Thermal and chemical approaches for oxygen catalytic recombination evaluation on ceramic materials at high temperature. *Applied Surface Science*, 120(3-4):225–238, 1997.

[4] P. F. Barbante. *Accurate and efficient modelling of high temperature nonequilibrium air flows*. PhD thesis, von Karman Institute for Fluid Dynamics / Université Libre de Bruxelles, 2001.

[5] P. F. Barbante and O. Chazot. Flight extrapolation of plasma wind tunnel stagnation region flowfield. *Journal of Thermophysics and Heat Transfer*, 20(3):493–499, July 2006.

[6] Larbi Bedra and Marianne Balat-Pichelin. Comparative modeling study and experimental results of atomic oxygen recombination on silica-based surfaces at high temperature. *Aerospace Science and Technology*, 9:318–328, June 2005.

[7] J. E. Broadwell. A simple model of the non-equilibrium dissociation of a gas in couette and boundary layer flows. *Journal of Fluid Mechanics*, 4(2):113–139, 1958.

[8] G. de Crombrugghe. Investigations of gas-surface interactions in plasma wind tunnels for catalycity characterization. Project report 2012-01, von Karman Institute for Fluid Dynamics, Rhode-Saint-Genèse, B1640, June 2012.

[9] R. Goulard. On catalytic recombination rates in hypersonic stagnation heat transfer. *Journal of Jet Propulsion*, 28(11):737–745, 1958.

[10] Roop N. Gupta, Jerrold M. Yos, Richard A. Thompson, and Kam-Pui Lee. A review of reaction rates and thermodynamic and transport properties for an 11-species air model for chemical and thermal nonequilibrium calculations to 30000k. Nasa-rp-1232, NASA Langley Research Center, Hampton, VA, United States, 1990.

[11] S. Herpin. Chemical aspects of hypersonic stagnation point heat transfer. Project report 2005-10, von Karman Institute for Fluid Dynamics, Rhode-Saint-Genèse, B1640, June 2005.

[12] A. F. Kolesnikov. Conditions of simulation of stagnation point heat transfer from a high-enthalpy flow. *Fluid Dynamics (from Russian)*, 28(1):131–137, 1993.

[13] H. W. Krassilchikoff. Procedure for the determination of the cold copper catalycity. Project report 2006-18, von Karman Institute for Fluid Dynamics, Rhode-Saint-Genèse, B1640, June 2006.

[14] Francesco Panerai. *Aerothermochemistry characterization of Thermal Protection Systems*. PhD thesis, von Karman Institute for Fluid Dynamics / Università Degli Studi Di Perugia, 2012.

DOI: 10.13009/EUCASS2019-103

[15] Daniel E. Rosner. Scale effects and correlations in nonequilibrium convective heat transfer. *AIAA Journal*, 1(7):1550–1555, July 1963.

[16] François Sanson, Nadège Villedieu, Francesco Panerai, Olivier Chazot, Pietro M. Congedo, and Thierry E. Magin. Quantification of uncertainty on the catalytic property of reusable thermal protection materials from high enthalpy experiments. *Experimental Thermal and Fluid Science*, 82:414 – 423, 2017.

[17] A. Viladegut. *Assessment of gas-surface interaction modelling for lifting body re-entry flight design*. PhD thesis, Universitat PolitÃ¨cnica de Catalunya/VKI, December 2017.

[18] Alan Viladegut, Ümran Düzel, and Olivier Chazot. Diffusion effects on the determination of surface catalysis in inductively coupled plasma facility. *Chemical Physics*, 485-486:88 – 97, 2017.